A Novel Salt Bridge Mechanism Highlights the Need for Nonmobile Proton Conditions to Promote Disulfide Bond Cleavage in Protonated Peptides Under Low-Energy Collisional Activation

Hadi Lioe[a,b] and Richard A. J. O'Hair[a,c]

[a] School of Chemistry, University of Melbourne, Melbourne, Australia
[b] Bio21 Institute of Molecular Science and Biotechnology, University of Melbourne, Melbourne, Australia
[c] ARC Centre of Excellence in Free Radical Chemistry and Biotechnology

The gas-phase fragmentation mechanisms of small models for peptides containing intermolecular disulfide links have been studied using a combination of tandem mass spectrometry experiments, isotopic labeling, structural labeling, accurate mass measurements of product ions, and theoretical calculations (at the MP2/6-311 + G(2d,p)//B3LYP/3-21G(d) level of theory). Cystine and its C-terminal derivatives were observed to fragment via a range of pathways, including loss of neutral molecules, amide bond cleavage, and S–S and C–S bond cleavages. Various mechanisms were considered to rationalize S–S and C–S bond cleavage processes, including charge directed neighboring group processes and nonmobile proton salt bridge mechanism. Three low-energy fragmentation pathways were identified from theoretical calculations on cystine N-methyl amide: (1) S–S bond cleavage dominated by a neighboring group process involving the C-terminal amide N to form either a protonated cysteine derivative or protonated sulfenyl amide product ion (44.3 kcal mol^{-1}); (2) C–S bond cleavage via a salt bridge mechanism, involving abstraction of the α-hydrogen by the N-terminal amino group to form a protonated thiocysteine derivative (35.0 kcal mol^{-1}); and (3) C–S bond cleavage via a Grob-like fragmentation process in which the nucleophilic N-terminal amino group forms a protonated dithiazolidine (57.9 kcal mol^{-1}). Interestingly, C–S bond cleavage by neighboring group processes have high activation barriers (63.1 kcal mol^{-1}) and are thus not expected to be accessible during low-energy CID experiments. In comparison to the energetics of simple amide bond cleavage, these S–S and C–S bond cleavage reactions are higher in energy, which helps rationalize why bond cleavage processes involving the disulfide bond are rarely observed for low-energy CID of peptides with mobile proton(s) containing intermolecular disulfide bonds. On the other hand, the absence of a mobile proton appears to "switch on" disulfide bond cleavage reactions, which can be rationalized by the salt bridge mechanism. This potentially has important ramifications in explaining the prevalence of disulfide bond cleavage in singly protonated peptides under MALDI conditions. (J Am Soc Mass Spectrom 2007, 18, 1109–1123) © 2007 American Society for Mass Spectrometry

Side chain cleavage reactions can compete with, and sometimes dominate over, sequence ion formation in the tandem mass spectra of protonated [1, 2] and deprotonated [3] peptides. Given that over 300 post-translational modifications (PTM) had been identified [4], these reactions can greatly help identify post-translationally modified residues via the loss of diagnostic small molecules. For example, the losses of H_3PO_4 [5] and CH_3SOH [6, 7] in the MS/MS of protonated peptides are indicators of phosphorylation and methionine sulfoxide formation, respectively. Progress has been made in understanding the factors that govern these reactions through a combination of mechanistic studies [1, 2, 6, 8] and interrogation of databases of tandem mass spectra [7]. Several different types of mechanisms may operate depending on the structure and properties of the peptide. For example, studies on simple derivatives of O-phosphoserine reveal that H_3PO_4 loss can occur via the following: charge directed neighboring group process (path A of Scheme **1**, X = H_2PO_4); and charge remote internal elimination reaction to form a dehydroalanine residue (path B of Scheme **1**, X = H_2PO_4) [8]. These different pathways can

This article is Part 54 of the series "Gas Phase Ion Chemistry of Biomolecules."

Presented in part at the 54th American Society for Mass Spectrometry (ASMS) Conference, Seattle, Washington, May 28–June 1, 2006.

Address reprint requests to Professor Richard O'Hair, School of Chemistry, University of Melbourne, Parkville, Victoria 3010, Australia. E-mail: rohair@unimelb.edu.au

1044-0305/07/$32.00
doi:10.1016/j.jasms.2007.03.003

Published online April 26, 2007
Received February 22, 2007
Revised March 8, 2007
Accepted March 9, 2007

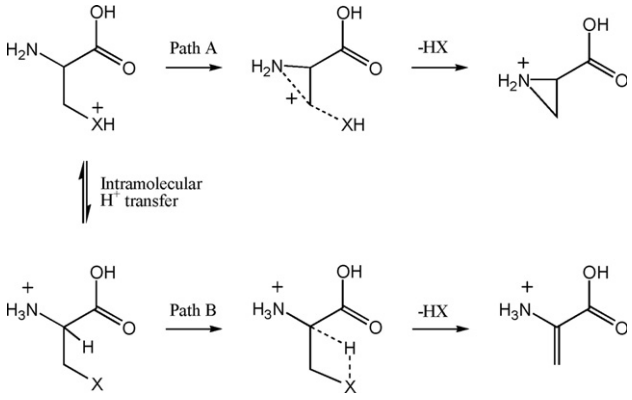

Scheme 1

be experimentally distinguished via deuterium labeling studies, and theoretical calculations provide information on the relative energies of the potential energy surfaces of these reactions. For example, in O-phosphoserine, when all exchangeable hydrogens are replaced by deuterium, D_3PO_4 is lost, indicating that the neighboring group process operates. Theoretical calculations also confirm that the barrier to the neighboring group process is lower in energy.

Another interesting class of side-chain cleavage reactions involving PTM is disulfide bond cleavage. Unlike O-phosphoserine and methionine sulfoxide, however, disulfide bond cleavage is generally not readily observed under low-energy CID conditions, hindering the identification of primary structure of peptides, especially if the peptide is contained within the disulfide loop [9]. Although there has been considerable interest in developing methods to target and cleave disulfide bonds in peptides [10–14], remarkably little work has been carried out to establish what factors govern disulfide bond cleavage, (which can either involve S–S or C–S bond cleavage), in the low-energy CID spectra of protonated peptides. It has been noted by Jones et al. [15] and McLuckey [16] that the abundance of disulfide bond cleavage is dependent on the number of charges on the peptide. For example, the $[M + 4H]^{4+}$ and $[M + 5H]^{5+}$ ions of insulin exclusively fragment via peptide bond cleavage, whereas the $[M + H]^+$ ion fragments via competitive disulfide bond cleavage and C-terminal glutamic acid amide bond cleavage [16]. Thus, the absence of a mobile proton [17, 18] appears to facilitate disulfide bond cleavage. The mechanistic features of these bond cleavage reactions have not been well established, although we were intrigued by a recent report [19], which proposed that S–S bond cleavage leads to the formation of a sulfenylium ion ($R\text{-}S^+$) and that C–S bond cleavage forms the $R\text{-}S\text{-}S^+$ product ion. Given that RS^+ cations are not very stable [20], the formation of cyclic product ions via neighboring group processes [6] seemed more likely.

Here we investigate disulfide bond cleavage reactions in small models for peptides containing intermolecular disulfide links under conditions of low-energy collision induced dissociation (CID). A combination of physical organic chemistry tools was utilized, including isotopic labeling, structural labeling, accurate mass measurements of product ions, and DFT calculations. The latter provide insights into the fragmentation mechanisms of S–S and C–S bond cleavage reactions. Various mechanisms for S–S and C–S bond cleavage reactions were interrogated and their relative likelihood of occurring was determined via a comparison of the energetics associated with the reactions coordinates for the model system, cystine N-methyl amide. Finally, the energetic requirement to cleave the disulfide bonds of model peptides were compared with that of amide bond cleavage processes.

Experimental

Materials

The disulfide bond cleavage reactions were studied using model systems of cysteine (Cys), cysteine derivatives (CysOMe, CysNHMe, AcCys, NMeCys, AcCysOMe, AcCysNHMe, AcCG), and cysteine-containing small peptides (CG, GC, GCG, GGC, GSSG). All reagents were also used as supplied: Cys, CysOMe, AcCys, (AcCysOMe)-$_{2-}$, and GSSG were purchased from Sigma-Aldrich (St. Louis, MO); CG, GC, GCG, and GGC were purchased from BaChem (Bubendorf, Switzerland); and D_2-cysteine [$H_2NCH(CD_2SH)CO_2H$ (98% D)] was obtained from Cambridge Isotope Laboratories. N-methyl cysteine was available from a previous study [21].

Modifications of Cysteine and Cysteine Derivatives

N-acetylation and O-methyl esterification of cysteine derivatives. We have used the general procedure for N-acetylation and O-Methyl esterification of amino acids and peptides [22].

N-methyl amidation of cysteine and cystine derivatives. We have used the method of Feenstra et al. [23] for methyl amidation of cysteine and cystine derivatives from the methyl ester. Briefly, 2 mg of the methyl ester of cysteine and cystine derivatives were dissolved in 1 mL of 30% aqueous CH_3NH_2 solution and the reaction was allowed to proceed at room temperature for 30 min. The mixture was dried by freeze drying, dissolved in 50% CH_3OH/50% H_2O containing 0.1 M acetic acid, and then lyophilized again. The methyl amide was used without further purification.

Oxidation of Cysteine Derivatives to Cystine Derivatives

Individual solutions of peptide containing cysteine residue were auto-oxidized in a 10 mM aqueous solution for 7 days to its *cystine* counterpart. Although we have not followed the auto-oxidation kinetics, these reactions essentially proceeded to completion, as judged by ESI

mass spectra. They were then diluted to a final total concentration of ~0.1 mM in 50% CH_3OH/50% H_2O solution containing 0.1 M acetic acid.

Mass Spectrometry Experiments

All experiments were carried out using a modified commercial ion trap mass spectrometer equipped with electrospray ionization (ESI) (Finnigan-MAT LCQ Classic; ThermoElectron Corp., San Jose, CA). The samples were introduced to the mass spectrometer at a flow rate of 3 μL/min. The sheath air, capillary voltage, and temperature were adjusted to ca. 30-60, 4.5 to 5.0 kV, and 180 °C, respectively. The CID experiments were performed using standard procedures by mass selecting the desired precursor ion, with an activation window of 2 to 3 *m/z*, and then subjecting it to CID using normalized collision energy of 12.5 to 18.5% and an activation Q of 0.25 for a period of 30 ms.

High-Resolution Mass Spectrometry Experiments

All high-resolution mass spectrometry experiments were conducted using a commercially available hybrid linear ion trap and Fourier transform ion cyclotron resonance (FT-ICR) mass spectrometer (Finnigan LTQ-FT; ThermoElectron Corp.), which is equipped with ESI. The samples were introduced to the mass spectrometer via direct injection through electrospray ionization using a flow rate of 3.5 μL/min. The sheath air, capillary voltage, and temperature were adjusted to ca. 2.5 to 25, 4.0 to 4.5 kV, and 275 °C, respectively. The CID experiments were performed in the linear ion trap by using standard procedures of mass selecting the desired precursor ion, with an activation window of 2.5 to 2.9 *m/z*, and then subjecting it to CID using a corresponding normalized collision energy of 25 to 34% and an activation Q of 0.25 for a period of 30 ms. The product ions were then analyzed in the FT-ICR MS to generate the high-resolution tandem mass spectrum. The instrument was externally calibrated using the standard calibration solution recommended by the manufacturer (a mixture of caffeine, MRFA, and Ultramark 1621) and standard procedure before analysis. All product ions of interest register a relative error in their exact masses of <0.7 ppm when compared with their predicted molecular formulas.

Calculation of Percentage of Different Bond Cleavages

We have used the formula shown in eq 1 to calculate S–S and C–S bond cleavage processes and "other bond cleavage" processes. The latter processes comprise of neutral molecule elimination and amide bond cleavage. X–X bond cleavage corresponds to specific bond cleavage process together with any product ions arising from subsequent fragmentation. We have not used the high-resolution MS data to calculate ion abundance as there appears to be a time-of-flight effect that results in discrimination of low mass ions.

$$\%\ \text{of X – X bond cleavage from MS/MS experiment} = (\Sigma\ \text{ion abundance for X – X bond cleaveage})/(\Sigma\ \text{all product ion abundance}) \times 100\% \quad (1)$$

Theoretical Calculations

Due to the large size of the system, it was not feasible to optimize all species on the potential energy surfaces for the competing fragmentation reactions of protonated cystine N-methyl amide at the B3LYP/6-31 + G(d,p) level of theory. Thus, a survey of different levels of theory was carried out on the model systems [$H_3NCH(CH_2SSX)CONHMe$] (X = H and CH_3). We established that single point energy calculations at the MP2/6-311 + G(2d,p) on B3LYP/3-21G(d) optimized structures with B3LYP/3-21G(d) zero point energy corrections gave similar results to those of the much more computationally expensive B3LYP/6-31 + G(d,p) optimizations and zero point energy corrections. Geometry optimizations for minima and transition states were carried out using the Gaussian 03 [24] molecular modeling package to gain further insights into different mechanisms by calculating the transition-state structures. Transition-state structures were connected to the minima using standard intrinsic reaction coordinate (IRC) calculations. The single point energy of all structures were further calculated at the MP2/6-311 + G(2d,p) level of theory [25]. All optimized structures were subjected to vibrational frequency analysis to confirm that the optimized structures are local/global minima (no imaginary frequency) or transition state (one imaginary frequency) and visualized using the computer package GaussView 3.0 [26].

The supplementary material is available in the electronic version of this article for:

(1) high-resolution MS/MS spectra of protonated $(CysOH)_2$, $(CysOMe)_2$, $(CysNHMe)_2$, and $(CG)_2$;
(2) CID MS/MS of some cystine derivatives;
(3) optimized structures for other calculated pathways to cleave S–S bond (path SSA and SSC) and C–S bond (path CSA, CSB, CS_gB, and CS_gC);
(4) complete structural details for each of the B3LYP/3-21G(d) optimized structures.

Results and Discussion

Fragmentation Studies of Cystine Derivatives, $(X\text{-}Cys\text{-}Y)_2$ (X = H, Y = OH, OMe, and NHMe) and Cystine-Containing Simple Peptides, $(CG)_2$, $(GC)_2$, $(GCG)_2$, and $(GCR)_2$

The CID spectra of protonated cystine [$(CysOH)_2$], several derivatives of cystine, and a number of cystine-

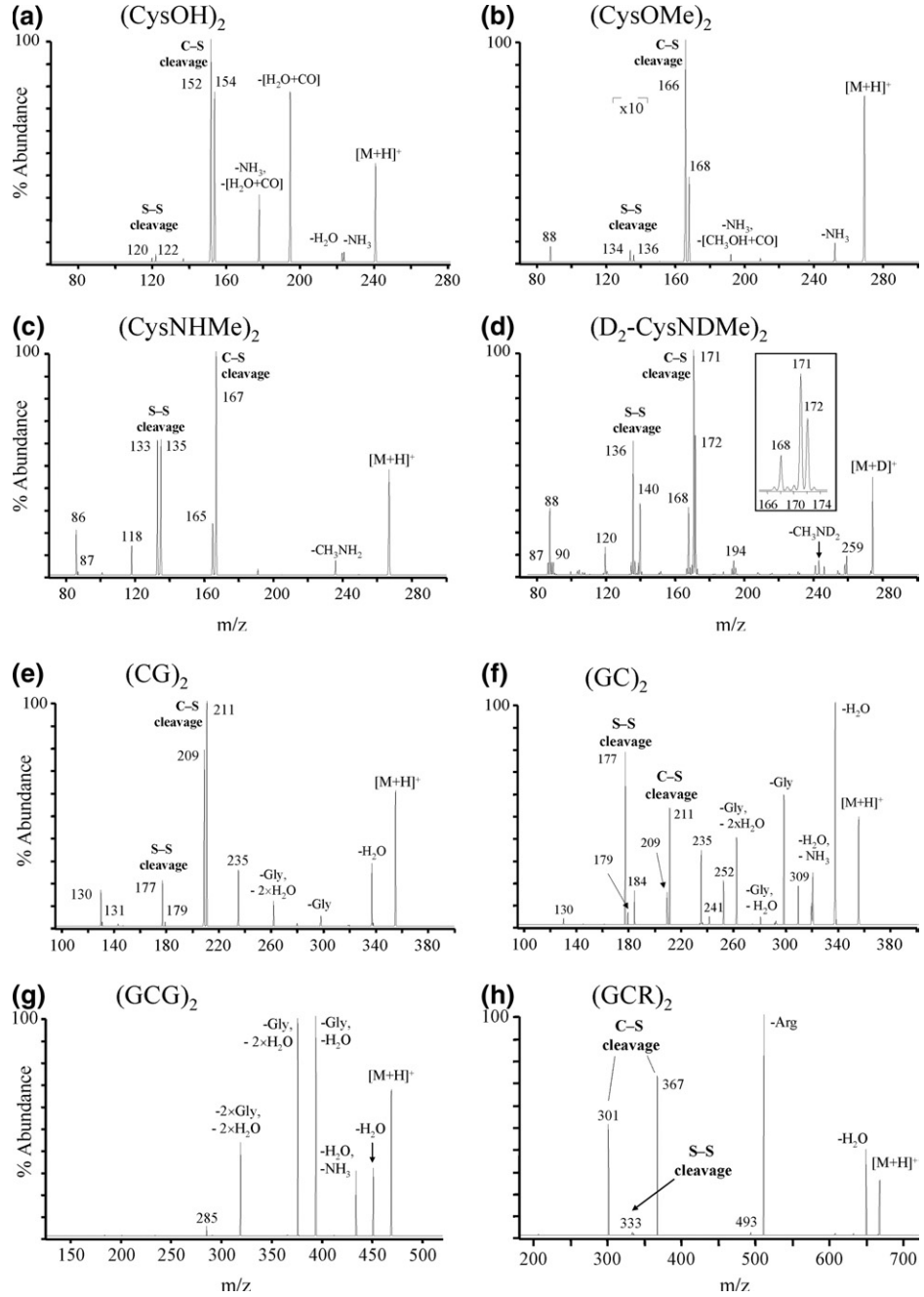

Figure 1. CID MS/MS spectra of cystine and its simple C-terminal derivatives and cystine-containing peptides: (**a**) $[M + H]^+$ of $(CysOH)_2$, (**b**) $[M + H]^+$ of $(CysOMe)_2$, (**c**) $[M + H]^+$ of $(CysNHMe)_2$, (**d**) $[M + D]^+$ of $(D_2\text{-}CysNDMe)_2$, (**e**) $[M + H]^+$ $(CG)_2$, (**f**) $[M + H]^+$ of $(GC)_2$, (**g**) $[M + H]^+$ of $(GCG)_2$, and (**h**) $[M + H]^+$ of $(GCR)_2$. For $(D_2\text{–}CysNDMe)_2$ the experiment was performed under H/D exchange conditions, whereby all acidic hydrogens were substituted with deuterium, leaving only the α-hydrogen. The insert shown in Figure 1(d) shows the expanded region for C–S bond cleavage.

containing peptides are shown in Figure 1. In addition, the CID spectra of several other cystine derivatives and cystine-containing peptides are shown in the supplementary material. For cystine (Figure 1a), several simple neutral molecule losses are observed, including losses of NH_3, H_2O, $[H_2O + CO]$, and $NH_3 + [H_2O + CO]$. In addition, product ions at *m/z* 120 and 122, and *m/z* 152 and 154 are observed, and these arise from S–S and C–S bond cleavage, respectively. This was further confirmed from accurate mass measurements (Figures S1a–d see supplementary Figures S1a–d), where it was found that these product ions have molecular formulas consistent with symmetric S–S and asymmetric C–S bond cleavage processes. The modified

C-terminal cystine derivatives (Figure 1b, c, and e) fragment in a similar fashion with the formation of product ions due to S–S and C–S bond cleavage being shifted to higher *m/z* values attributable to the C-terminal modification [e.g., for $(CysOMe)_2$ these product ions are shifted upfield by 14Da, for $(CysNHMe)_2$ by 13Da, and for $(CG)_2$ by 57Da]. For $(CysOMe)_2$ and $(CysNHMe)_2$ the formation of the S–S and C–S fragment ions almost dominate the MS/MS spectra.

Isotopic labeling studies of $(D_2\text{-}CysNHMe)_2$, where all hydrogen except for α-hydrogen has been substituted with deuterium to form $(D_2\text{-}CysNDMe)_2$, shows a small amount of scrambling occurring before fragmentation, as indicated by a series of product ions that form the triplets (centered at *m/z* 88, 136, 168, and 194) shown in Figure 1d. More interestingly, C–S bond cleavage process undergoes more extensive scrambling to form the unexpected but dominant product ion at *m/z* 171. The insert in Figure 1d shows the expanded region of the C–S bond cleavage process. Hence, the C–S bond cleavage reaction appears to involve the α-hydrogen.

Figure 1f–h shows the MS/MS spectra of simple peptides containing cystine, in which the disulfide bond is not at the N-terminal of the peptide. Unlike the other cystine derivatives shown in Figure 1a–e where the disulfide bond is at the N-terminus, the fragmentation is dominated by neutral molecule losses and amide bond cleavages. In addition, with the exception of protonated $(GC)_2$ shown in Figure 1f, S–S and C–S bond cleavage processes are absent. This fragmentation behavior is consistent with the observation that disulfide bond cleavage in the fragmentation of larger tryptic peptides containing disulfide bond are rarely observed [9], suggesting that disulfide bond cleavage processes have higher relative energy barriers compared with amide bond cleavages. This example is best illustrated by the fragmentation of protonated $(GCG)_2$, which fragments under low-energy CID to mainly eliminate small molecules and various combinations of glycyl residue and H_2O (Figure 1g). When fragmentation occurs under nonmobile proton condition, as in the case of protonated $(GCR)_2$, C–S bond cleavage is readily observed (*m/z* 367 and 301) (see Figure 1h). The only other fragmentation processes observed are H_2O loss, loss of Arg residue, and a very small amount of S–S bond cleavage. Thus, the absence of a mobile proton appears to have a profound influence on disulfide bond cleavage.

The fragmentation of all cystine derivatives studied are summarized in Table 1, showing the percentage of processes due to S–S bond cleavage, C–S bond cleavage, and other bond cleavage processes (small neutral loss and amide bond cleavage). It can be seen from Table 1 that most disulfide bond cleavage reactions (S–S and C–S bond cleavages) are observed only for the small cystine derivatives, especially if the disulfide bond is at the N-terminus. To provide further insights into disulfide bond cleavage reactions, and to understand why disulfide bonds are not easily cleaved for large peptides with mobile proton(s), we performed theoretical calculations to investigate the different fragmentation pathways, and these are described in later sections.

Table 1. Percentage of bond cleavage in the CID fragmentation of all peptides studied that contain a cystine moiety

Peptide derivatives	% of S–S bond cleavage	% of C–S bond cleavage	% of other processes
$(Cys)_2$	1.8	58.8	39.4
$(CysOMe)_2$	0.5	90.4	9.0
$(CysNHMe)_2$	46.9	49.4	3.7
$(NMeCysOH)_2$	0.0	100	0.0
$(AcCysOH)_2$	0.0	0.0	100.0
$(AcCysOMe)_2$	1.1	0.0	98.9
$(AcCysNHMe)_2$	0.0	0.0	100.0
$(AcCG)_2$	0.0	0.0	100.0
$(CG)_2$	8.0	67.7	24.3
$(GC)_2$	17.2	14.6	68.2
$(GCG)_2$	0.0	0.0	100.0
$(GGC)_2$	0.0	0.0	100.0
GSSG	0.0	0.0	100.0
$(GCR)_2$	0.9	46.5	52.6

Various Mechanisms for S–S and C–S Bond Cleavage Reactions

Since our previous studies had demonstrated that charge directed neighboring group processes are energetically favorable for amino acid and peptide ion fragmentation [8, 27, 28], we proposed a similar mechanism for S–S bond cleavage processes shown in Scheme **2**, i.e., neighboring group attack by N-terminal amino N (path SSA), C-terminal amide N (path SSB), or C-terminal carbonyl O (path SSC) to γ-sulfur of S-protonated $(CysX)_2$, where X = OH, OMe, NHMe, or Gly. During the S–S bond cleavage process an ion-molecule complex [29] is formed during which proton transfer process can occur to form cyclic product ions (**C**), (**E**), or (**F**), or protonated cysteine derivative (**D**), depending on the proton affinity of the individual neutral fragment [30]. We should note that these bond cleavage processes are preceded by an intramolecular proton transfer from N-terminal amino group to the disulfide group, which unfortunately could not be located at the B3LYP/3-21G(d) level of theory. However, it is expected that the intramolecular proton transfer process to be lower in energy than bond cleavage processes. It should be noted that Structure **F** is related to one of the neutral structures previously proposed for S–S bond cleavage products [19].

For C–S bond cleavage, we proposed three competing mechanisms: (1) charge directed neighboring group processes summarized in Scheme **3**, (2) fragmentation involving the formation of salt bridge intermediate shown in Scheme **4**, and (3) charge directed Grob-type fragmentation [31, 32] summarized in Scheme **5**. For charge directed neighboring group mechanisms shown in Scheme **3**, C–S bond cleavage is effected by nucleophilic attack by either the: N-terminal amino N (path

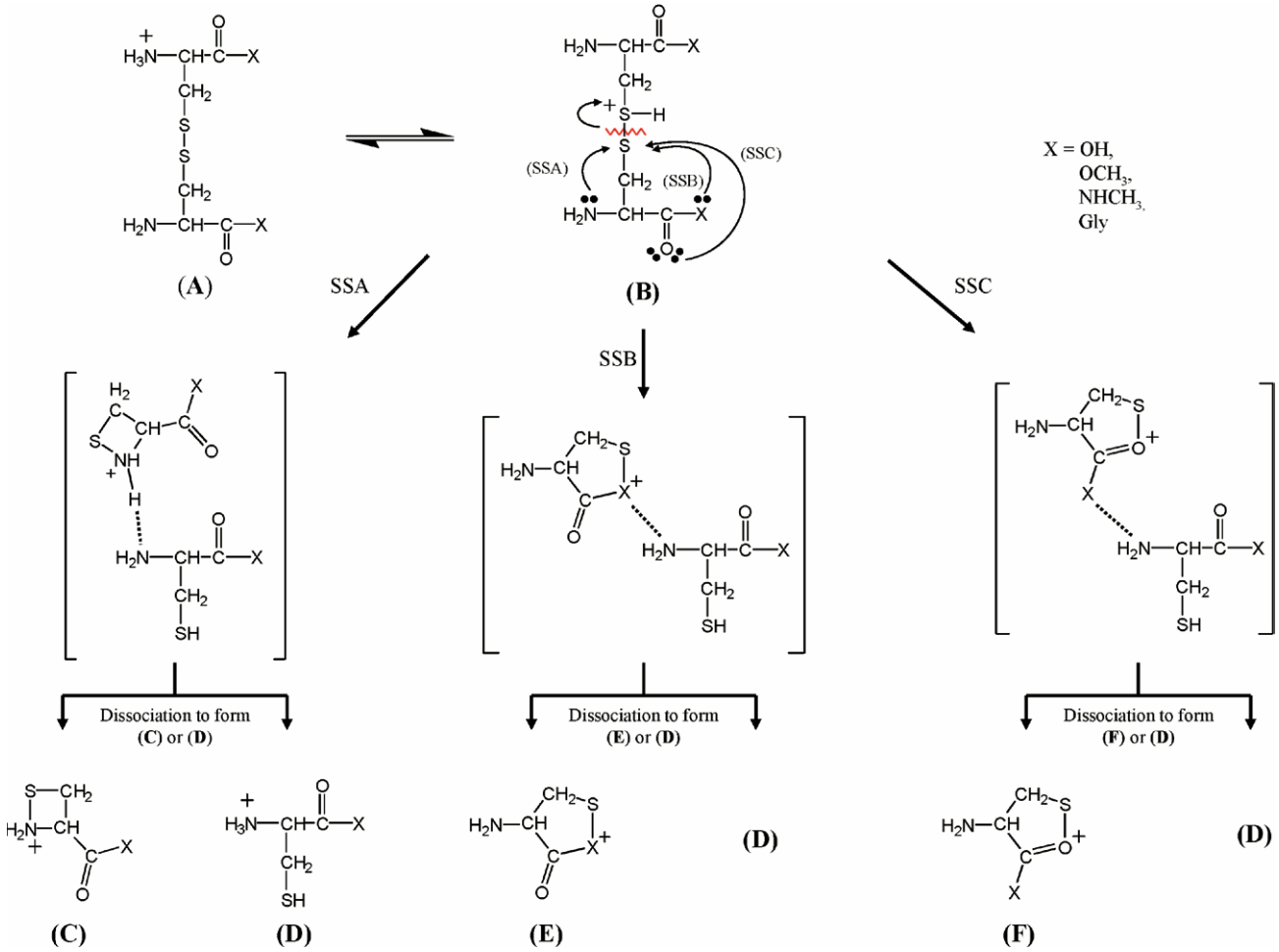

Scheme 2. S–S (NG).

CSA) (c.f. path A of Scheme **1**); C–terminal amide N (path CSB); or C-terminal carbonyl O (path CSC) to β-carbon of S-protonated cystine derivative. These reactions form cyclic product ions (**G**), (**I**), or (**J**), or protonated S-thio-cysteine derivative (**H**).

To explain the scrambling observed in C–S bond cleavage in deuterated $(D_2$-CysNDMe$)_2$ (Figure 1d), we proposed a mechanism to cleave the C–S bond, which involves the α-hydrogen before fragmentation (Scheme **4**). In this mechanism, C–S bond cleavage is instigated by abstraction of the α-hydrogen by the basic N-terminal amino group from the opposite backbone, which forms a salt bridge ion-molecule complex. Intramolecular proton transfer within the ion-molecule complex would then yield either protonated dehydroalanine derivative (Structure **K**) or protonated S-thio-cysteine derivative (**H**). For this mechanism, the charge is located at the N-terminal amino group and is not involved in the bond cleavage reaction. Abstraction of the α-hydrogen by the C-terminal carbonyl O was not considered due to lower basicity of the carbonyl group compared with amino functional group [PA(methyl amine) = 214.9 kcal mol^{-1} versus PA(methyl acetamide) = 212.4 kcal mol^{-1}][33]. This mechanism is in fact a variant of path B of Scheme **1**, but with a stronger base and less steric constraint (4-membered ring versus 8-membered ring transition state).

The C–S bond cleavage mechanism shown in Scheme **5** is similar to condensed phase Grob fragmentation [31, 32], where the nucleophile is the N-terminal amino N (path CS_gA), C-terminal amide N (path CS_gB), or C-terminal carbonyl O (path CS_gC), to form cyclic disulfide product ions (**L**), (**M**), or (**N**), respectively. A combination of two neutrals, (an acrylic acid derivative and NH_3) are eliminated during this fragmentation process. In the next sections we model the various competing S–S and C–S bond cleavage processes using theoretical calculations; these competing mechanisms were then compared with each other and with amide bond cleavage processes.

Computational Studies on Disulfide Bond Cleavage Reactions

We have modeled the S–S and C–S bond cleavage reactions using $(CysNHMe)_2$ at the B3LYP/3-21G(d)

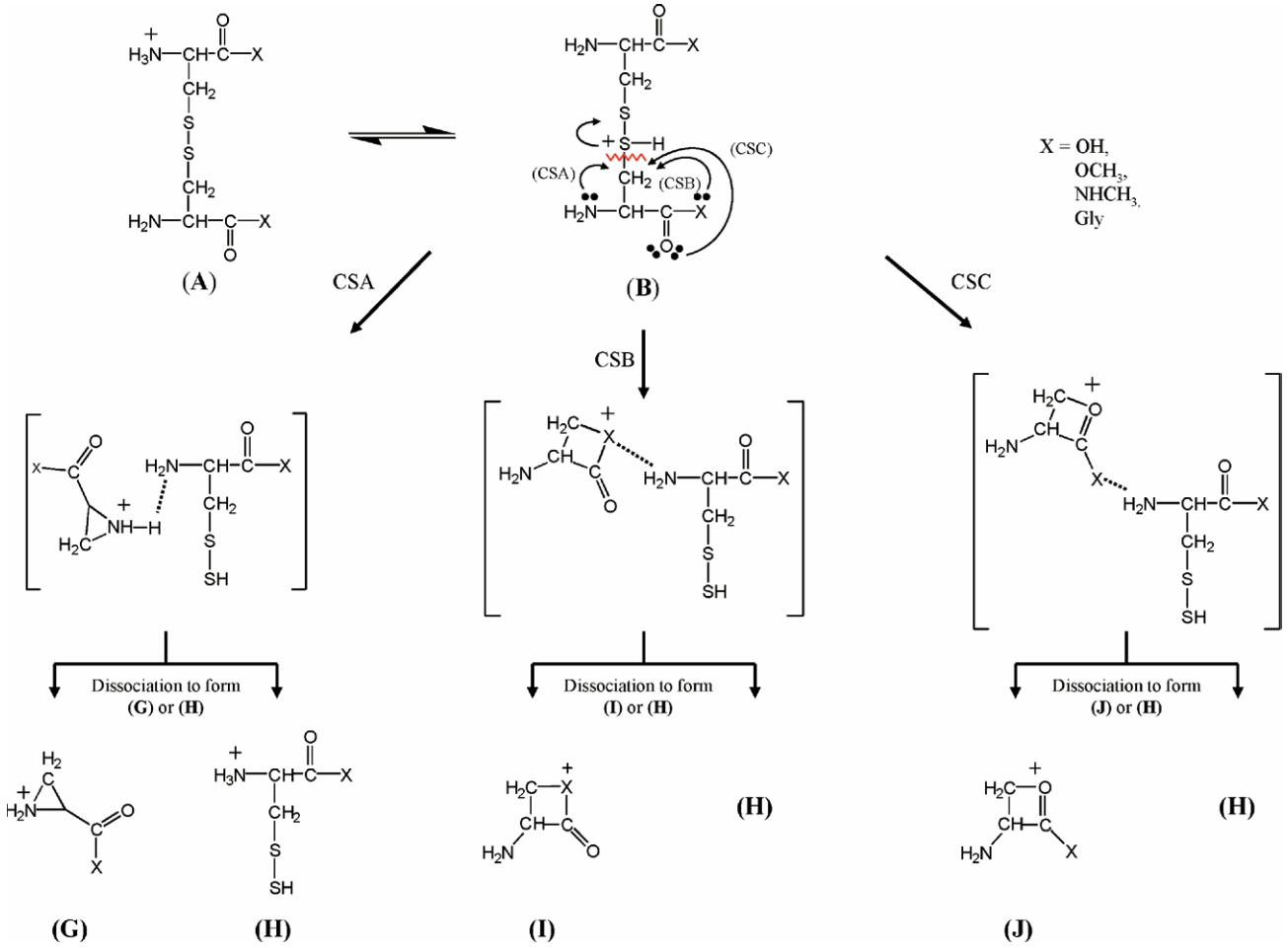

Scheme 3. C–S (NG).

level of theory, and the single point energy was further calculated at the MP2/6-311 + G(2d,p)//B3LYP/3-21G(d) level of theory.

S–S Bond Cleavage Reaction by Neighboring Group Processes

Figure 2 shows the optimized structures for the most energetically preferable pathway for breaking S–S bond (path SSB in Scheme **2**) at the B3LYP/3-21G(d) level of theory, including the relative energies (relative to the global minimum Structure **A**), which were calculated at the MP2/6-311 + G(2d,p)//B3LYP/3-21G(d) level of theory. In this pathway, S–S bond cleavage is effected by nucleophilic attack by C-terminal amide N to form either a protonated sulfenyl amide (Structure **E**) or protonated cysteine N-methyl amide (Structure **D**). This pathway has a calculated transition-state energy of +40.3 kcal mol^{-1} (**TS-SSB** in Figure 2). However, the endothermicity (ΔE_R) of the reaction to form protonated sulfenyl amide (**E**) and neutral cysteine-N-methyl amide CysNHMe was predicted to be slightly higher at +44.7 kcal mol^{-1}. On the other hand, the energy of reaction (ΔE_R) is lower at +37.5 kcal mol^{-1} if proton transfer occurred within the ion-molecule complex [29] to form protonated CysNHMe (Structure **D**) and neutral sulfenyl amide. Interestingly, related sulfenyl amide structures have previously been proposed as intermediates in the regulation of cysteine dependent enzyme, the protein tyrosine phosphatase 1B [34, 35]. It should be noted that sulfenyl amide (**E**) is protonated at the N-terminal amino group, which cannot be formed by simple separation of ion-molecule complex after transition-state **TS-SSB** (Figure 2). Instead, it is formed by a second subsequent intramolecular proton transfer process from protonated CysNHMe. This process is related to the proton transport catalyzed isomerization reactions described by Bohme [36]. The endothermicity for formation of protonated sulfenyl amide by simple bond lengthening from the ion-molecule complex was calculated to be very high at +63.3 kcal mol^{-1} (data not shown).

Structures **E** and **D** are possible product ion structures for *m/z* 133 and 135 observed in the MS/MS of protonated $(CysNHMe)_2$, respectively (Figure 1c). Since the endothermicities for the formation of both product ions are close to the transition-state energy, the formation of both product ions is accessible with equal probability during CID of protonated $(CysNHMe)_2$. The optimized structures for species related in other path-

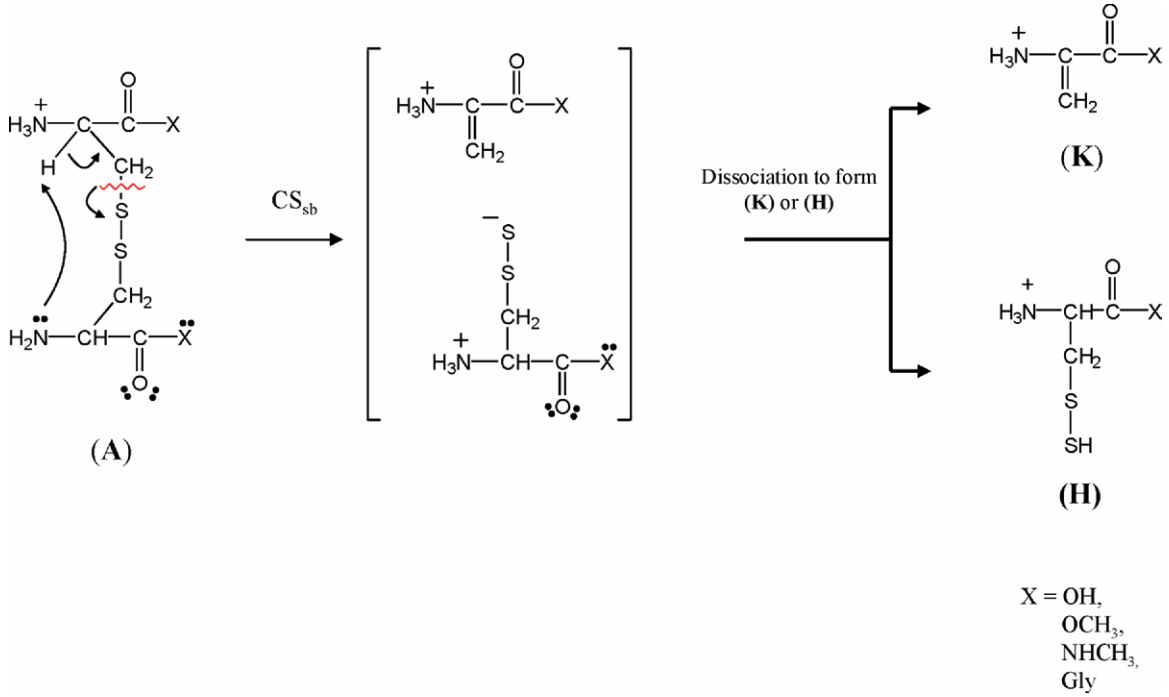

Scheme 4. C–S (salt bridge).

ways (paths SSA and SSC) are shown in Figures S3 and S4 supplementary Figures S3 and S4, respectively.

C–S Bond Cleavage Reaction by Neighboring Group Processes

Figure 3 shows the optimized structures and their relative energies (relative to the global minimum Structure **A**) for the lowest energy pathway to breaking the C–S bond via charge directed neighboring group mechanism (path CSC shown in Scheme **3**). In path CSC, C–S bond cleavage is effected by nucleophilic attack of β-carbon by C-terminal carbonyl O to form a 4-membered cyclic product ion (Structure **J**), with a predicted transition-state barrier of 55.9 kcal mol^{-1}. It is interesting to note that this mechanism does not involve S-protonated $(CysNHMe)_2$ structure. Instead, transition-state **TS-CSC** is a concerted transition state for intramolecular proton transfer from C-terminal carbonyl O to disulfide group and nucleophilic attack to form the 4-membered product

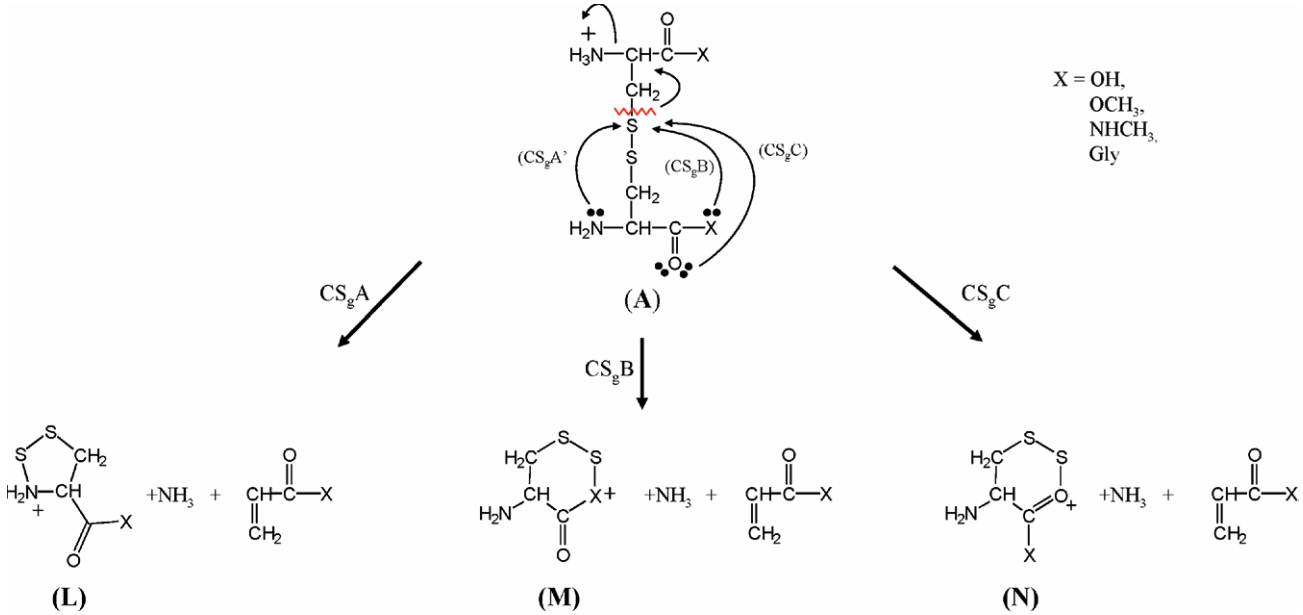

Scheme 5. C–S (Grob).

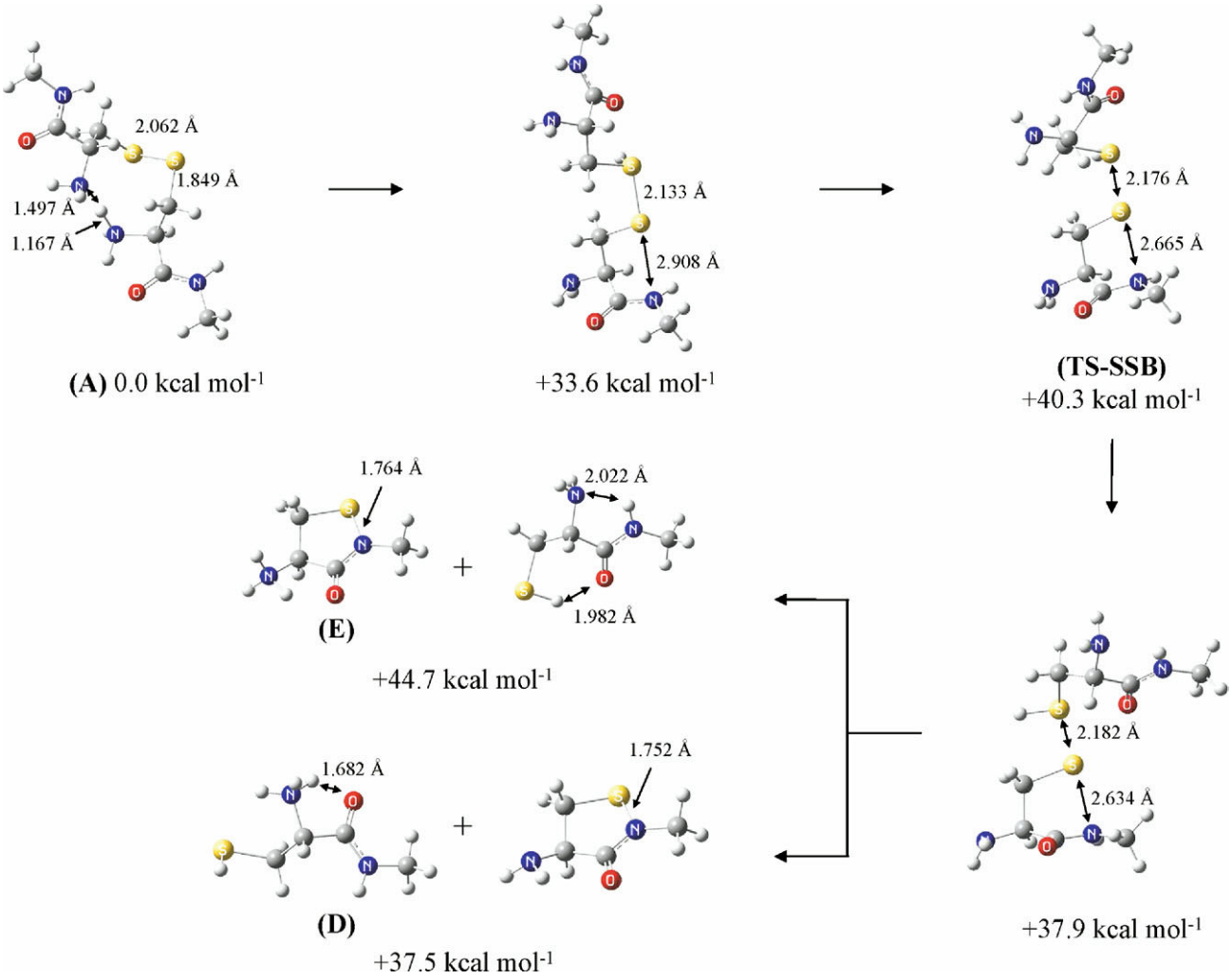

Figure 2. MP2/6-311 + G(2d,p)//B3LYP/3-21G(d) optimized structures and relative energies showing the reaction coordinate for the lowest energy pathway for S–S bond cleavage via neighboring group attack by C-terminal amide N (pathway SSB shown in Scheme **2**). All reported energy values are relative to global minimum **A**. All other pathways in Scheme **2** (pathways SSA and SSC) are shown in Figures S2 and S3 supplementary Figures S2 and S3.

ion. Due to the strain in the 4-membered ring product ion Structure **J**, this pathway has a very high endothermicity (ΔE_R) of +63.1 kcal mol^{-1}. The product of intramolecular proton transfer to form protonated thiocysteine N-methyl amide (Structure **H**) also has a high endothermicity (ΔE_R) of +64.0 kcal mol^{-1}. Due to the high-energy barrier for this process, this mechanism is expected to be insignificant in C–S bond cleavage. The optimized structures and relative energies of the other higher energy pathways CSA and CSB are shown in Figures S5 and S6 supplementary Figures S5 and S6, respectively.

C–S Bond Cleavage Reaction by Salt Bridge Mechanism

The salt bridge mechanism to cleave C–S bond is similar to the *cis*- elimination shown in path B of Scheme **1**, but with a stronger base and larger transition-state ring size. In this mechanism (CS_{sb} shown in Scheme **4**) bond cleavage is induced by abstraction of α-hydrogen, which weakens the C–S bond and forms a salt bridge intermediate. Additionally, the charge is remote from the reaction centre (N-protonated) and is not involved in the salt bridge mechanism.

Figure 4 shows the optimized structures for all species involved in this salt bridge mechanism. This pathway has a transition-state energy of +35.5 kcal mol^{-1}, and the energy of the reaction (ΔE_R) is +44.2 kcal mol^{-1}, forming protonated dehydroalanine N-methyl amide (Structure **K**) and neutral thiocysteine N-methyl amide. However, intramolecular proton transfer within the ion-molecule complex can form protonated thiocysteine N-methyl amide (Structure **H**) and neutral dehydroalanine N-methyl amide with a lower endothermicity (ΔE_R) at +34.4 kcal mol^{-1}. Due to

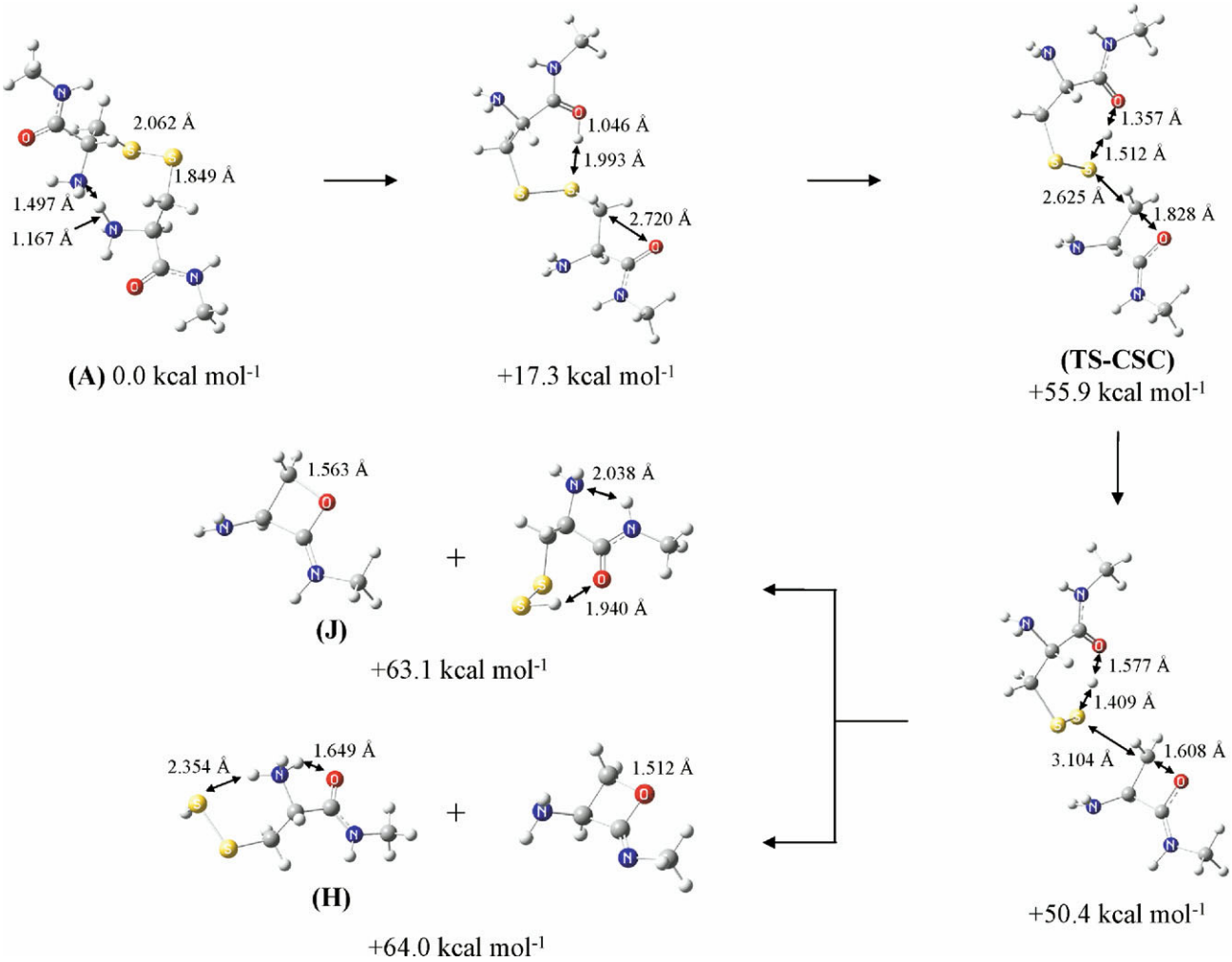

Figure 3. MP2/6-311 + G(2d,p)//B3LYP/3-21G(d) optimized structures and relative energies showing the reaction coordinate for the lowest energy pathway for C–S bond cleavage via neighboring group attack by C-terminal carbonyl O (pathway CSC shown in Scheme **3**. All reported energy values are relative to global minimum **A**. All other pathways in Scheme **3** (pathways CSA and CSB) are shown in Figures S4 and S5 supplementary Figures S4 and S5.

the low endothermicity for the formation of Structure **H**, the salt bridge mechanism is expected to only form *m/z* 167 product ion under low-energy CID MS/MS of $(CysNHMe)_2$ (Figure 1c). Furthermore, since the α-hydrogen has been transferred to the N-thiocysteine methyl amide fragment, this mechanism is consistent with the extensive scrambling observed before formation of thiocysteine N-methyl amide from fragmentation of isotopically labeled $(D_2\text{-CysNDMe})_2$ (see Figure 1d) and an earlier section for more details about the scrambling of α-hydrogen).

Additionally, since the salt bridge mechanism has a much lower energy barrier (+35.0 kcal mol^{-1}) compared with the neighboring group mechanism, it is expected to be the dominant fragmentation mechanism to explain the C–S bond cleavage forming the product ion at *m/z* 167. Furthermore, this mechanism is triggered by the abstraction of α-hydrogen by the basic N-terminal amino group. Thus, increasing the basicity of the N-terminal amino group is expected to decrease the energy barrier for this energetically preferable process. As shown in the fragmentation of protonated $(NMeCysOH)_2$, exclusive cleavage of the C–S bond is observed to form thiocysteine product ion (see supplementary Figure S2b for the CID MS/MS data of protonated $(NMeCysOH)_2$). Thus, this shows that fragmentation can be readily manipulated by chemical derivatization.

C–S bond cleavage can also be enhanced by restricting the mobility of the ionizing proton, as clearly demonstrated in the fragmentation of protonated $(GCR)_2$ (Figure 1h). Abundant C–S bond cleavage to form the protonated thiocysteine derivative (*m/z* 367) and the dehydroalanine derivative (*m/z* 301) is observed in the MS/MS spectrum. Since one of the Arg residues in $(GCG)_2$ is expected to sequester the ionizing proton, fragmentation occurs under nonmobile proton conditions. In addition, the other Arg residue is more basic than the N-terminal amino group

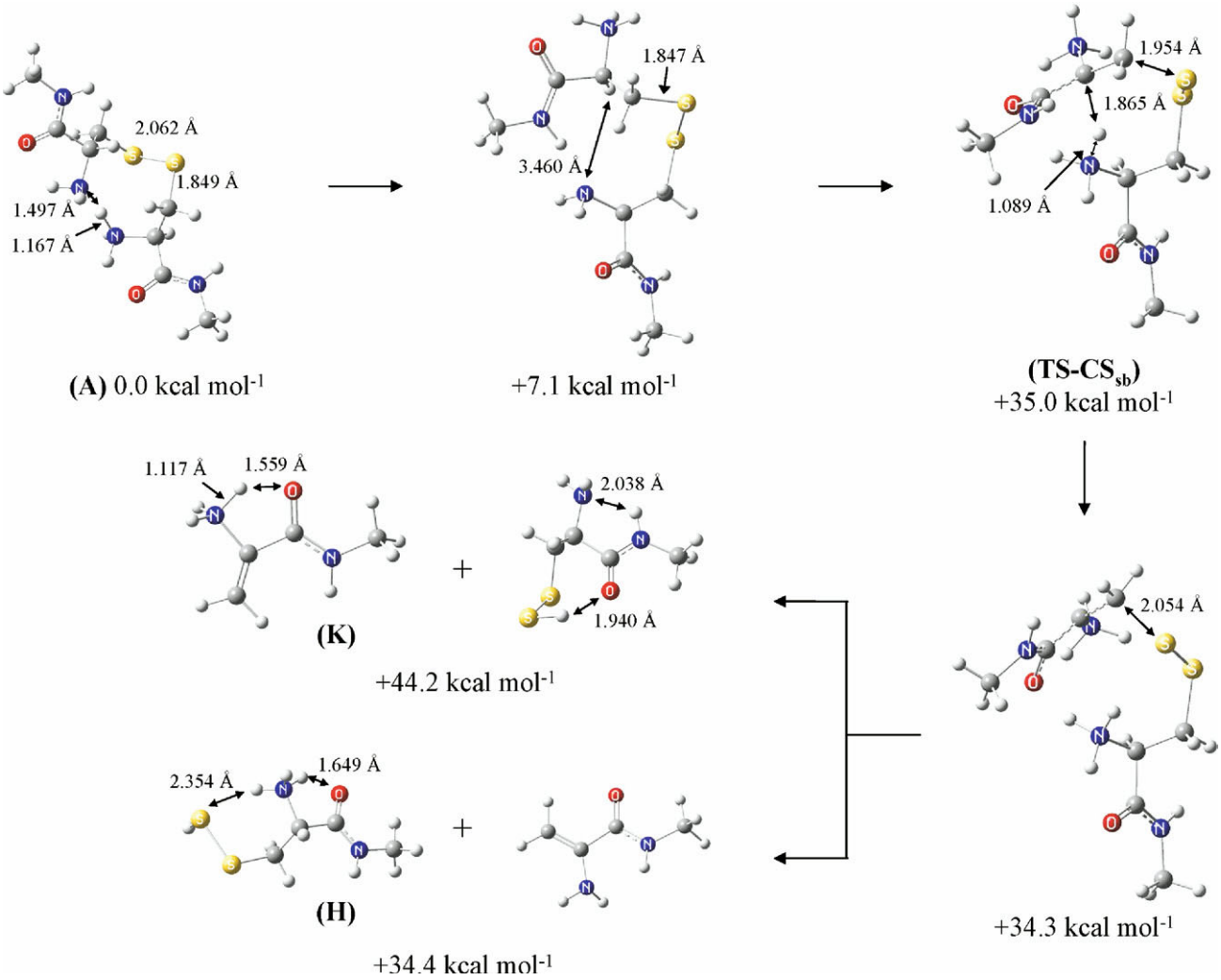

Figure 4. MP2/6-311 + G(2d,p)//B3LYP/3-21G(d) optimized structures and relative energies showing the reaction coordinate for the lowest energy pathway for C–S bond cleavage via salt bridge mechanism (pathway CS_{sb} shown in Scheme **4**). All reported energy values are relative to global minimum **A**.

and is expected to play an important role in the abstraction of the α-hydrogen.

C–S Bond Cleavage Reaction by Grob Fragmentation Mechanism

Figure 5 shows the optimized structure for all species involved in the lowest energy pathway for Grob fragmentation mechanism for C–S bond cleavage. This lowest energy pathway proceeds via nucleophilic attack by N-terminal amino N to disulfide group to form dithiazolidine product ion (Structure **L**) and eliminating methylacrylamide and NH_3. The transition-state energy for this process was predicted to be +56.1 kcal mol^{-1}, and the endothermicity of the reaction (ΔE_R) was predicted to be +57.9 kcal mol^{-1}, clearly higher than the energy barrier for S–S bond cleavage via neighboring group mechanism (+40.3 kcal mol^{-1} for path SSB) and C–S bond cleavage via salt bridge mechanism (+35.0 kcal mol^{-1}). Since product ion Structure **L** is a possible candidate for a product ion structure for *m/z* 165 in the MS/MS of protonated $(CysNHMe)_2$ (see Figure 1c), the higher energy barrier for the Grob-type fragmentation mechanism is consistent with the small abundance of this product ion. The optimized structures and relative energies of the other higher energy pathways CS_gB and CS_gC are shown in Figures S7 and S8 supplementary Figures S7 and S8, respectively.

Summary of the Lowest Energy Pathways for S–S and C–S Bond Cleavage

All the transition-state energies for various competing S–S and C–S bond cleavage reactions, including the fragmentation pathways shown in the supplementary materials, are summarized in Table 2. The energies of reaction (ΔE_R) for each pathway are also included in Table 2. As can be seen from Table 2,

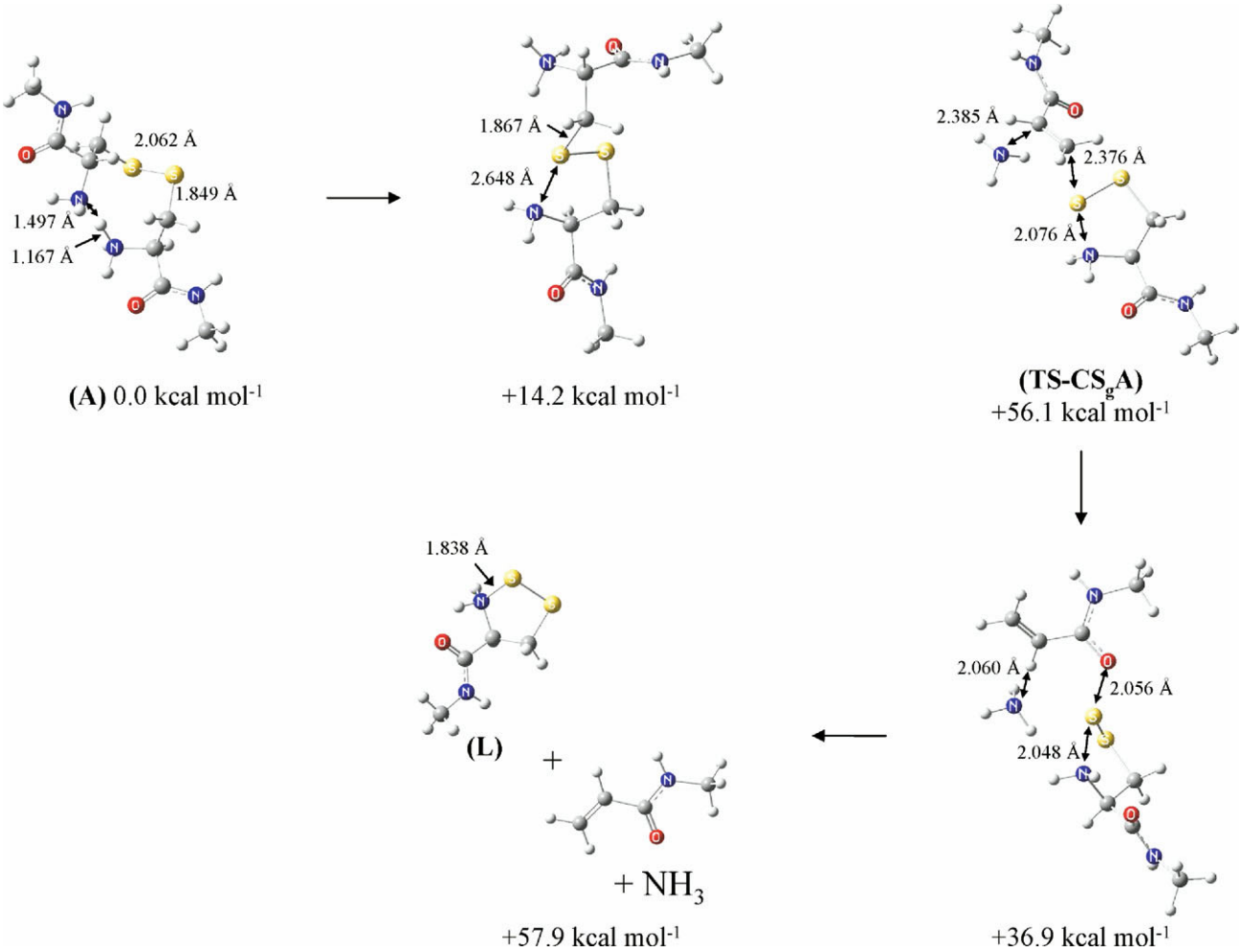

Figure 5. MP2/6-311 + G(2d,p)//B3LYP/3-21G(d) optimized structures and relative energies showing the reaction coordinate for the lowest energy pathway for C–S bond cleavage via Grob-type fragmentation whereby the N-terminal amino N acts as the intramolecular nucleophile (pathway CS_gA shown in Scheme **5**. All reported energy values are relative to global minimum **A**. All other pathways in Scheme **5** (pathways CS_gB and CS_gC) are shown in supplementary Figures S6 and S7.

some pathways have a higher endothermicity than the transition state, while additional proton transfer step within ion-molecule complexes lowers the endothermicity considerably for other pathways. We also have underlined the lowest energy pathway for each mechanism (S–S or C–S bond cleavage) to indicate the

Table 2. Calculated transition energy barrier ($\Delta E^{\ddagger}$) and the relative energy of the separated products (ΔE_R) in parentheses for the competing bond cleavage processes in model system protonated $(Cys\text{-}NHMe)_2$

	$\Delta E^{\ddagger}$, kcal mol^{-1} (ΔE_R, kcal mol^{-1})[a]		
Types of bond cleavage processes	Amino-N	Amide-N	Carbonyl-O
(1) S–S bond cleavage (NG mechanism)[b]	38.5 (58.5, 58.4)	<u>40.3 (44.7, 37.5)</u>	32.2 (54.0, 60.6)
(2) C–S bond cleavage (NG mechanism)[c]	76.5 (53.8, 49.9)	70.6 (64.7, 43.8)	<u>55.9 (63.1, 64.0)</u>
(3) C–S bond cleavage (salt-bridge mechanism)[d]	<u>35.0 (34.4, 44.2)</u>	—	—
(4) C–S bond cleavage (Grob fragmentation)[e]	<u>56.1 (57.9)</u>	70.8 (74.7)	60.2 (66.4)
(5) Amide bond cleavage		25–40[f]	

[a]The underlined numbers signify the pathway with the lowest energy for each mechanism.
[b]S–S bond cleavage via neighboring group process with various nucleophiles (see Scheme 2).
[c]C–S bond cleavage via neighboring group process with various nucleophiles (see Scheme 3).
[d]C–S bond cleavage via salt-bridge mechanism (see Scheme 4).
[e]C–S bond cleavage via Grob fragmentation using with nucleophiles (see Scheme 5).
[f]Range of typical values cited in reference [33].

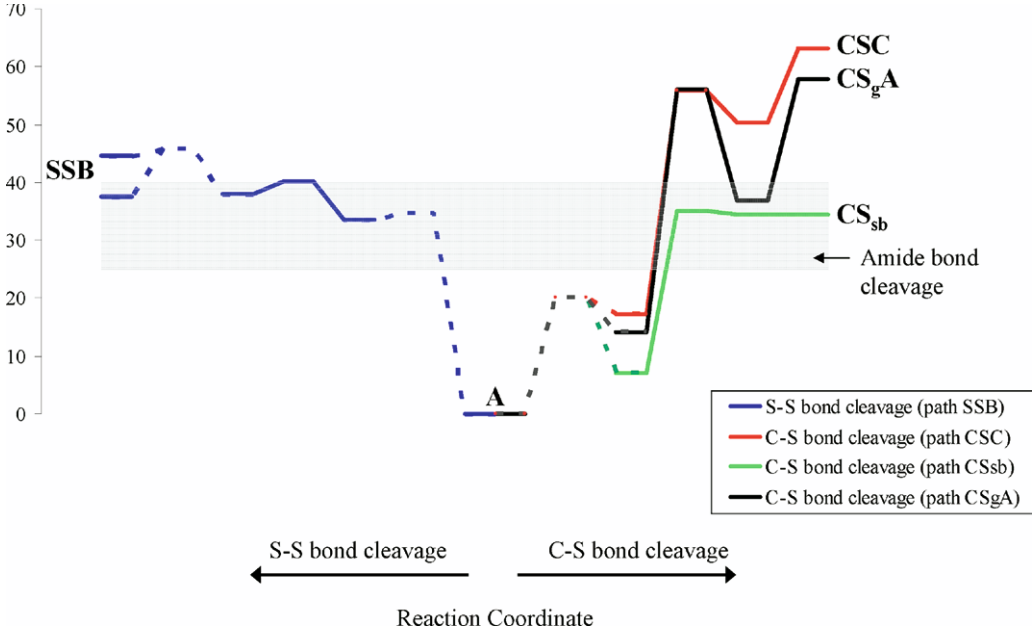

Figure 6. The MP2/6-311 + G(2d,p)//B3LYP/3-21G(d) calculated potential energy surfaces (PES) for competing fragmentation pathways of protonated $(CysNHMe)_2$. This PES summarizes only the lowest energy pathways for each fragmentation mechanisms shown in Schemes **2–5**, and the optimized structures are shown in Figures 3–6). All energies are relative to the global minimum Structure **A**. Path SSB to cleave S–S bond via neighboring group mechanism is represented by the blue PES, path CSC to cleave C–S bond via neighboring group mechanism is shown in the red PES, path CS_{sb} to cleave C–S bond via salt bridge mechanism is shown in the green PES, and path CS_gA to cleave C–S bond via Grob-type fragmentation mechanism is shown in black PES. Dashed lines represent transition states (that were not located) interconnecting conformers.

most probable pathway that can occur from each fragmentation mechanism. These results are also summarized in Figure 6, which shows the lowest energy potential energy surfaces from each fragmentation mechanism (both S–S and C–S bond cleavage). It should be noted that some transition states for bond rotations and intramolecular proton transfer processes were not calculated, and are thus represented by dotted lines.

For all the mechanisms considered, path CS_{sb} to cleave the C–S bond is the lowest energy process and is expected to dominate the fragmentation pathway. This is consistent with the CID spectrum of $(CysNHMe)_2$, which shows the formation of thiocysteine N-methyl amide at *m/z* 167 to be the most dominant product ion. S–S bond cleavage process by neighboring group (path SSB) is also expected to be a dominant process due to its rather low-energy barrier. This is also highlighted in the abundant formation of protonated sulfenyl amide (*m/z* 133) and protonated CysNHMe (*m/z* 135) in the MS/MS spectrum of $(CysNHMe)_2$ (Figure 1c). The Grob-like fragmentation mechanism (path CS_gA) is expected to form a small abundance of dithiazolidine product ion due to the reasonably high-energy barrier for this process. Finally, the neighboring group process to cleave C–S bond (path CSC) is expected not to operate due to the high-energy barrier of the process.

When Will Disulfide Bond Cleavage Occur?

From Table 2 and Figure 6, clearly there are various competing pathways for S–S and C–S bond cleavage processes, which can complicate the fragmentation behavior of protonated peptide containing disulfide bonds. However, these competing processes are in fact much higher in energy than typical amide bond cleavages. For example, in Figure 6 the typical energetic requirement to cleave amide bonds or eliminate neutral molecules [37] were included as a band of energy between 25 to 40 kcal mol^{-1}. As can be seen in Figure 6, most disulfide bond cleavage processes (S–S and C–S bond cleavage) lie outside the band of energy required to cleave an amide bond in a peptide, with the exception of the salt bridge mechanism to cleave the C–S bond. This is further illustrated in the CID MS/MS fragmentation of the heterodimer of AcCysNHMe-CysNHMe, linked by a disulfide bond (see supplementary Figure S2c). In this system, various fragmentation processes can occur under CID, including amide, S–S, and C–S bond cleavages. However fragmentation is dominated by amide bond cleavage via elimination of CH_3NH_2, and no disulfide bond cleavage is observed (see supplementary Figure S2c).

How then, can disulfide bond cleavage reactions be promoted in larger peptides? Clearly for this to happen, access to an enolate anion is desirable. This can be achieved in two ways: (1) via negative ion CID experi-

ment [38, 39], as recently demonstrated in a joint experimental and theoretical study by Bowie and coworkers [40,41]; and (2) in protonated peptides that have nonmobile protons, thereby promoting the salt bridge mechanism (c.f. Scheme **4**). Interestingly, this last factor might explain the prevalence of disulfide bond cleavage in MALDI experiment [15].

Conclusions

Cystine and its C-terminal derivatives and simple peptides containing intermolecular disulfide bonds fragment via a variety of pathways, including losses of neutral molecules, amide bond cleavage, and S–S and C–S bond cleavages. Various mechanisms were considered to explain S–S and C–S bond cleavage processes, including charge directed neighboring group processes and nonmobile proton fragmentation processes. Using theoretical calculations performed on protonated $(CysNHMe)_2$ (at the MP2/6-311 + G(2d,p)//B3LYP/3-21G(d) level of theory) three low-energy fragmentation pathways were identified, which should be energetically accessible during low-energy CID MS/MS experiments: (1) S–S bond cleavage dominated by a neighboring group process involving C-terminal amide N to form either protonated CysNHMe (*m/z* 135) or protonated sulfenyl amide product ion (*m/z* 133) (path SSB of Scheme **2**); (2) C–S bond cleavage process is dominated via a salt bridge mechanism, involving the α-hydrogen to form protonated thiocysteine N-methyl amide (*m/z* 167) (Scheme **4**); and [3] C–S bond cleavage process is also dominated by the Grob-like fragmentation where the nucleophile is the N-terminal amino group to form dithiazolidine product ion (*m/z* 165) (path CS_gA of Scheme **5**). Interestingly C–S bond cleavage by neighboring group processes (Scheme **3**) have high-energy barriers and are expected to be inaccessible energetically during CID MS/MS experiment. In comparison to simple amide bond cleavage, these processes are higher in energy, explaining why disulfide bond cleavage processes are rarely observed for low-energy CID fragmentation of peptide ions containing disulfide bonds which have mobile proton(s).

This study highlights the complexity of fragmentation reactions for even such a small system as the cystine derivative, $(CysNHMe)_2$. In fact, the disulfide bond brings a range of potentially reactive functional groups (nucleophile and electrophile) into close proximity, allowing different reactions to compete. The presence of an intermolecular disulfide bond also allows other fragmentation pathways such as the salt bridge mechanism to occur, which are uncommon in amino acids and simple di- or tripeptides [42]. In this work, product ion stabilities were shown to be an important factor in determining the lowest energy fragmentation pathway. Finally, this study further highlights the importance of the role of mobile proton in dictating the types of fragmentation reactions observed under low-energy CID. Disulfide bond cleavage reactions in protonated peptides join the pantheon of nonmobile proton reactions, which include C-terminal aspartic acid (and to a lesser extent glutamic acid cleavage) [43,44] and CH_3SOH loss from methionine sulfoxide-containing peptides [6,7].

Acknowledgments

The authors thank ARC for financial support via grant DP0558430 (to RAJO) and the ARC Centre of Excellence in Free Radical Chemistry and Biotechnology. They thank VICS for the Chemical Sciences High Performance Computing Facility, and Dr. Gavin Reid for helpful discussions. HL acknowledges the award of an Elizabeth and Vernon Puzey Postgraduate Scholarship.

References

1. O'Hair, R. A. J. The Role of Nucleophile- Electrophile Interactions in the Unimolecular and Bimolecular Gas-Phase Ion Chemistry of Peptides and Related Systems. *J. Mass Spectrom.* **2000,** *35*, 1377–1381.
2. Paizs, B.; Suhai, S. Fragmentation Pathways of Protonated Peptides. *Mass Spectrom. Rev.* **2005,** *24*, 508–548.
3. Bowie, J. H.; Brinkworth, C. S.; Dua, S. Collision-Induced Fragmentations of the $[M - H]^-$ Parent Anions of Underivatized Peptides: An Aid to Structure Determination and Some Unusual Negative Ion Cleavages. *Mass Spectrom. Rev.* **2002,** *21*, 87–107.
4. Jensen, O. N. Modification-Specific Proteomics: Characterization of Post-Translational Modifications by Mass Spectrometry. *Curr. Op. Chem. Biol.* **2004,** *8*, 33–41.
5. Mann, M.; Jensen, O. N. Proteomic Analysis of Post-Translational Modifications. *Nat. Biotech.* **2003,** *21*, 255–261.
6. O'Hair, R. A. J.; Reid, G. E. Neighboring Group Versus *cis*-Elimination Mechanisms for Side Chain Loss from Protonated Methionine, Methionine Sulfoxide, and Their Peptides. *Eur. J. Mass Spectrom.* **1999,** *5*, 325–334.
7. Reid, G. E.; Roberts, K. D.; Kapp, E. A.; Simpson, R. J. Statistical and Mechanistic Approaches to Understanding the Gas-Phase Fragmentation Behavior of Methionine Sulfoxide Containing Peptides. *J. Proteome Res.* **2004,** *3*, 751–759.
8. Reid, G. E.; Simpson, R. J.; O'Hair, R. A. J. Leaving Group and Gas Phase Neighboring Group Effects in the Side Chain Losses from Protonated Serine and Its Derivatives. *J. Am. Soc. Mass Spectrom.* **2000,** *11*, 1047–1060.
9. Gorman, J. J.; Wallis, T. P.; Pitt, J. J. Protein Disulfide Bond Determination by Mass Spectrometry. *Mass Spectrom. Rev.* **2002,** *21*, 183–216.
10. Zubarev, R. A.; Kruger, N. A.; Fridriksson, E. K.; Lewis, M. A.; Horn, D. M.; Carpenter, B. K.; McLafferty, F. W. Electron Capture Dissociation of Gaseous Multiply-Charged Proteins is Favored at Disulfide Bonds and Other Sites of High Hydrogen Atom Affinity. *J. Am. Chem. Soc.* **1999,** *121*, 2857–2862.
11. Fung, Y. M. E.; Kjeldsen, F.; Silivra, O. A.; Chan, T. W. D.; Zubarev, R. A. Facile Disulfide Bond Cleavage in Gaseous Peptide and Protein Cations by Ultraviolet Photodissociation at 157 nm. *Angew. Chem. Int. Ed.* **2005,** *44*, 6399–6403.
12. Gunawardena, H. P.; O'Hair, R. A. J.; McLuckey, S. A. Selective Disulfide Bond Cleavage in Gold(I) Cationized Polypeptide Ions Formed via Gas-Phase Ion/Ion Cation Switching. *J. Proteome Res.* **2006,** *5*, 2087–2092.
13. Loo, J. A.; Edmonds, C. G.; Udseth, H. R.; Smith, R. D. Effect of Reducing Disulfide-Containing Proteins on Electrospray Ionization Mass Spectra. *Anal. Chem.* **1990,** *62*, 693–698.
14. Wu, J.; Watson, J. T. A Novel Methodology for Assignment of Disulfide Bond Pairings in Proteins. *Prot. Sci.* **1997,** *6*, 391–398.
15. Jones, M. D.; Patterson, S. D.; Lu, H. S. Determination of Disulfide Bonds in Highly Bridged Disulfide-Linked Peptides by Matrix-Assisted Laser Desorption/Ionization Mass Spectrometry with Postsource Decay. *Anal. Chem.* **1998,** *70*, 136–143.
16. Wells, J. M.; Stephenson, J. L.; McLuckey, S. A. Charge Dependence of Protonated Insulin Decompositions. *Int. J. Mass Spectrom.* **2000,** *203*, A1–A9.
17. Wysocki, V. H.; Tsaprailis, G.; Smith, L. L.; Breci, L. A. Mobile and Localized Protons: A Framework for Understanding Peptide Dissociation. *J. Mass Spectrom.* **2000,** *35*, 1399–1406.
18. Kapp, E. A.; Schütz, F.; Reid, G. E.; Eddes, J. S.; Moritz, R. L.; O'Hair, R. A. J.; Speed, T. P.; Simpson, R. J. Mining a Tandem Mass Spectrometry Database To Determine the Trends and Global Factors Influencing Peptide Fragmentation. *Anal. Chem.* **2003,** *75*, 6251–6264.
19. Rubino, F. M.; Verduci, C.; Giampiccolo, R.; Pulvirenti, S.; Brambilla, G.; Colombi, A. Characterization of the Disulfides of Biothiols by Electrospray Ionization and Triple-Quadrupole Tandem Mass Spectrometry. *J. Mass Spectrom.* **2004,** *39*, 1408–1416.

20. de Moraes, P. R. P.; Linnert, H. V.; Aschi, M.; Riveros, J. M. Experimental and Theoretical Characterization of Long-Lived Triplet State $CH_3CH_2S^+$ Cations. *J. Am. Chem. Soc.* **2000,** *122*, 10133–10142.
21. Freitas, M. A.; O'Hair, R. A. J.; Williams, T. D. Gas-Phase Reactions of Cysteine with Charged Electrophiles: Regioselectivities of the Dimethylchlorinium Ion and the Methoxymethyl Cation. *J. Org. Chem.* **1997,** *62*, 6112–6120.
22. Reid, G. E.; Simpson, R. J.; O'Hair, R. A. J. A Mass Spectrometric and ab Initio Study of the Pathways for Dehydration of Simple Glycine and Cysteine-Containing Peptide $[M + H]^+$ Ions. *J. Am. Soc. Mass Spectrom.* **1998,** *9*, 945–956.
23. Feenstra, R. W.; Stokkingreef, E. H. M.; Reichwein, A. M.; Lousberg, W. B. H.; Ottenheijm, H. C. J. Oxidative Preparation of Optically Active N-Hydroxy-α-Amino Acid Amides. *Tetrahedron* **1990,** *46*, 1745–1756.
24. Frisch, M. J.; Trucks, G. W.; Schlegel, H. B.; Scuseria, G. E.; Robb, M. A.; Cheeseman, J. R.; Montgomery, J. A., Jr.; Vreven, T.; Kudin, K. N.; Burant, J. C.; Millam, J. M.; Iyengar, S. S.; Tomasi, J.; Barone, V.; Mennucci, B.; Cossi, M.; Scalmani, G.; Rega, N.; Petersson, G. A.; Nakatsuji, H.; Hada, M.; Ehara, M.; Toyota, K.; Fukuda, R.; Hasegawa, J.; Ishida, M.; Nakajima, T.; Honda, Y.; Kitao, O.; Nakai, H.; Klene, M.; Li, X.; Knox, J. E.; Hratchian, H. P.; Cross, J. B.; Adamo, C.; Jaramillo, J.; Gomperts, R.; Stratmann, R. E.; Yazyev, O.; Austin, A. J.; Cammi, R.; Pomelli, C.; Ochterski, J. W.; Ayala, P. Y.; Morokuma, K.; oth, G. A.; Salvador, P.; Dannenberg, J. J.; Zakrzewski, V. G.; Dapprich, S.; Daniels, A. D.; Strain, M. C.; Farkas, O.; Malick, D. K.; Rabuck, A. D.; Raghavachari, K.; Foresman, J. B.; Ortiz, J. V.; Cui, Q.; Baboul, A. G.; Clifford, S.; Cioslowski, J.; Stefanov, B. B.; Liu, G.; Liashenko, A.; Piskorz, P.; Komaromi, I.; Martin, R. L.; Fox, D. J.; Keith, T.; Al-Laham, M. A.; Peng, C. Y.; Nanayakkara, A.; Challacombe, M.; Gill, P. M. W.; Johnson, B.; Chen, W.; Wong, M. W.; Gonzalez, C.; Pople J. A. Gaussian 03 (Rev B.04); Gaussian, Inc.: Pittsburgh PA, 2003.
25. Turecek, F. Proton Affinity of Dimethyl Sulfoxide and Relative Stabilities of C_2H_6OS Molecules and $C_2H_7OS^+$ Ions. A Comparative G2(MP2) ab Initio and Density Functional Theory Study. *J. Phys. Chem. A* **1998,** *102*, 4703–4713.
26. Keith, T.; Millam, J.; Eppinnett, K.; Hovell, W. L.; Gilliland, R. *GaussView (Ver 3.0)* Dennington II, R.; Semichem, Inc.: Shawnee Mission, KS, 2003.
27. Lioe, H.; O'Hair, R. A. J.; Reid, G. E. Gas-Phase Reactions of Protonated Tryptophan. *J. Am. Soc. Mass Spectrom.* **2004,** *15*, 65–76.
28. Lioe, H.; O'Hair, R. A. J. Neighboring Group Processes in the Deamination of Protonated Phenylalanine Derivatives. *Org. Biomol. Chem.* **2005,** *3*, 3618–3628.
29. Bowen, R. D. Ion-Neutral Complexes. *Acc. Chem. Res.* **1991,** *24*, 364–371.
30. Morgan, D. G.; Bursey, M. M. A Linear Free-Energy Correlation in the Low-Energy Tandem Mass Spectra of Protonated Tripeptides Gly-Gly-Xxx. *Org. Mass Spectrom.* **1994,** *29*, 354–359.
31. Grob, C. A. Mechanisms and Stereochemistry of Heterolytic Fragmentation. A*ngew. Chem. Int. Ed.* **1969,** *8*, 535–546.
32. Kurti, L.; Czako, B. In *Strategic Applications of Named Reactions in Organic Synthesis: Background and Detailed Mechanisms*; Elsevier Academic: Burlington, 2005; p 190.
33. Hunter, E. P.; Lias, S. G. Proton Affinity Evaluation. In *NIST Chemistry WebBook, NIST Standard Reference Database Number 69*; Linstrom, P. J., Mallard, W. G.; National Institute of Standards and Technology: Gaithersburg, MD, 20899 (http://webbook.nist.gov/cgi/cbook.cgi?Contrib-), June 2005.
34. Salmeen, A.; Andersen Jannik, N.; Myers Michael, P.; Meng, T.-C.; Hinks John, A.; Tonks Nicholas, K.; Barford, D. Redox Regulation of Protein Tyrosine Phosphatase 1B Involves a Sulphenyl-Amide Intermediate. *Nature* **2003,** *423*, 769–773.
35. van Montfort-Rob, L. M.; Congreve, M.; Tisi, D.; Carr, R.; Jhoti, H. Oxidation State of the Active-Site Cysteine in Protein Tyrosine Phosphatase 1B. *Nature* **2003,** *423*, 773–777.
36. Bohme, D. K. Proton Transport in the Catalyzed Gas-Phase Isomerization of Protonated Molecules. *Int. J. Mass Spectrom. Ion Processes* **1992,** *115*, 95–110.
37. Amunugama, M.; Roberts, K. D.; Reid, G. E. Mechanisms for the Selective Gas-Phase Fragmentation Reactions of Methionine Side Chain Fixed Charge Sulfonium Ion Containing Peptides. *J. Am. Soc. Mass Spectrom.* **2006,** *17*, 1631–1642.
38. Zhou, J.; Ens, W.; Poppeschriemer, N.; Standing, K. G.; Westmore, J. B. Cleavage of Interchain Disulfide Bonds Following Matrix-Assisted Laser-Desorption. *Int. J. Mass Spectrom. Ion Processes* **1993,** *126*, 115–122.
39. Chrisman, P. A.; McLuckey, S. A. Dissociations of Disulfide-Linked Gaseous Polypeptide/Protein Anions: Ion Chemistry with Implications for Protein Identification and Characterization. *J. Proteome Res.* **2002,** *1*, 549–557.
40. Bilusich, D.; Maselli, V. M.; Brinkworth, C. S.; Samguina, T.; Lebedev, A. T.; Bowie, J. H. Direct Identification of Intramolecular Disulfide Links in Peptides Using Negative Ion Electrospray Mass Spectra of Underivatized Peptides. A Joint Experimental and Theoretical Study. *Rapid Commun. Mass Spectrom.* **2005,** *19*, 3063–3074.
41. Bilusich, D.; Bowie, J. H. Identification of Intermolecular Disulfide Linkages in Underivatized Peptides Using Negative Ion Electrospray Mass Spectrometry. A Joint Experimental and Theoretical Study. *Rapid Commun. Mass Spectrom.* **2007,** *21*, 619–628.
42. Farrugia, J. M.; O'Hair, R. A. J. Involvement of Salt Bridges in a Novel Gas-Phase Rearrangement of Protonated Arginine-Containing Dipeptides which Precedes Fragmentation. *Int. J. Mass Spectrom.* **2003,** *222*, 229–242.
43. Tsaprailis, G.; Nair, H.; Somogyi, A.; Wysocki, V. H.; Zhong, W.; Futrell, J. H.; Summerfield, S. G.; Gaskell, S. J. Influence of Secondary Structure on the Fragmentation of Protonated Peptides. *J. Am. Chem. Soc.* **1999,** *121*, 5142–5154.
44. Bailey, T. H.; Laskin, J.; Futrell, J. H. Energetics of Selective Cleavage at Acidic Residues Studied by Time- and Energy-Resolved Surface-Induced Dissociation in FT-ICR MS. *Int. J. Mass Spectrom.* **2003,** *222*, 313–327.